International Journal of Materials Science

E-ISSN: 2707-823X
P-ISSN: 2707-8221
Impact Factor (RJIF): 5.92
Journal's Website
IJMS 2026; 7(1): 107-115
Received: 15-10-2025
Accepted: 16-11-2025

Bhagwat M Fulmante
Department of Physics, Sanjeevanee Mahavidyalaya, Chapoli, Maharashtra, India

Waghmare Vaibhav Sanjiv
Department of Physics, Sanjeevanee Mahavidyalaya, Chapoli, Maharashtra, India

Corresponding Author:
Bhagwat M Fulmante
Department of Physics, Sanjeevanee Mahavidyalaya, Chapoli, Maharashtra, India

Green-synthesized defect-engineered nanomaterials for solar-driven water purification

Bhagwat M Fulmante and Waghmare Vaibhav Sanjiv

DOI: https://www.doi.org/10.22271/27078221.2026.v7.i1b.109

Abstract
Solar photocatalysis represents a viable low-cost solution to decentralized water purification, but the traditional photocatalysts are still subject to UV-activation and recombination of charge-carriers. In this work, a green-synthesized, defect-engineered heterojunction is suggested: oxygen-vacancy-rich TiO 2 - x is used together with porous g-C 3 N 4 nanosheets (PCN), to allow the removal of both dyes (methylene blue, rhodamine B) and pathogens (E. coli, S. aureus) upon solar power. The TiO 2 is formed and defects created through a plant-polyphenol pathway, which is then combined at low temperature with PCN to enhance harvesting of visible light and transfer of charge at the interface. The optimized composite (TiO 2-x/PCN-3) was found to be 95-99% in dye decolorization (pseudo-first-order kinetics) and >5-log bacteria inactivation under simulated sunlight (AM 1.5G) which was better than pristine TiO 2 and PCN controls. Scavenger experiments suggest that the oxidation of dye is predominantly affected by the presence of the radicals, which are: O 2 - and OH, whereas the attack on the membrane by ROS is controlling the activation of bacteria. The cost analysis alone indicates that the platform could be used in low resource deployment using immobilized films or coated substrates.

Keywords: Green synthesis, oxygen vacancies, TiO_2-x, g-C_3N_4, solar photocatalysis, dye degradation, photocatalytic disinfection

1. Introduction
Synthetic dye and microbial pathogen contamination of water are endemic environmental and human health issues, especially in those areas where industrial effluent and poor sanitation overlap. Dyes that are deliberately engineered to be resistant to fading, chemical attack and biodegradation are common in textile, leather, paper, and pharmaceutical effluents. Consequently, the wastewater containing the dye is capable of remaining in the water body decreasing light penetration, distorting photosynthesis, and increasing chemical oxygen demand. Simultaneously, pathogenic water microbes in the contaminated water resources cause wateraborne illness outbreaks, particularly when centralized treatment is not widespread or when the water distribution systems provide recontamination opportunities. These two threats encourage the invention of treatment technologies that would control both the degradation of organic pollutants and microorganisms without generating any harmful secondary wastes.

Semiconductor photocatalysis is one of the other advanced treatment methods that have received long term attention since it can theoretically mineralize organic pollutants and treat water with the aid of solar energy. The principle of it is that once a semiconductor receives photons of high enough energy, electrons are excited out of the valence band into the conduction band, leaving behind positively charged holes. These charge carriers formed in the process of photosynthesis undergo redox reactions with water and dissolved oxygen to produce reactive oxygen species (ROS) like hydroxyl radicals (•OH) and superoxide radicals (•O 2 -). Such ROS are capable of oxidizing dye molecules by successive intermediates to mineralization and of attacking cell walls, membranes and intracellular elements of a microorganism, resulting in inactivation (Hoffmann *et al.*, 1995) [21].

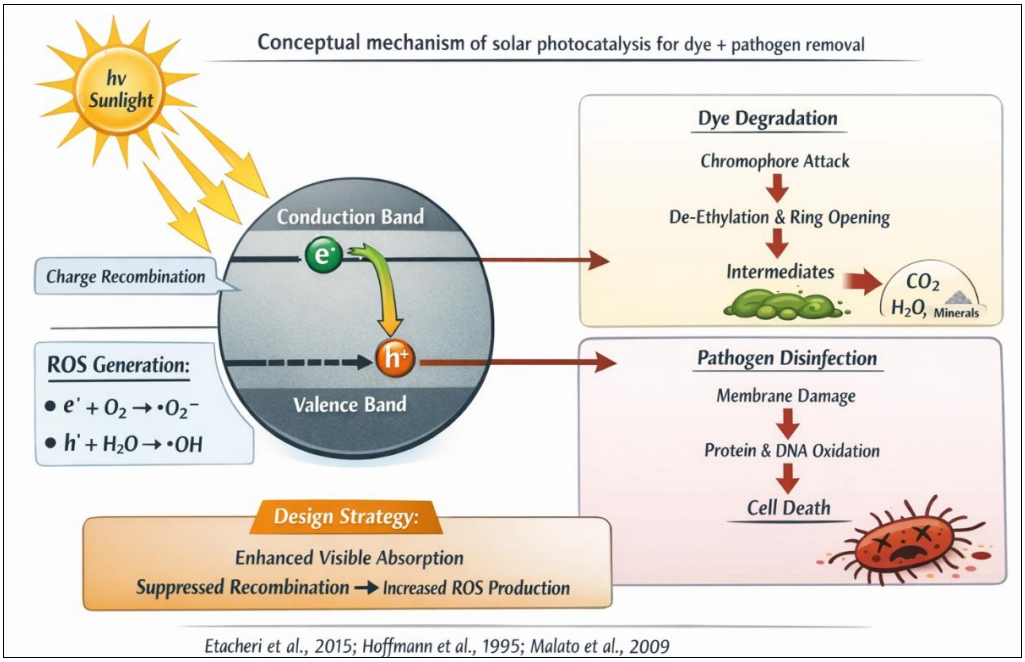

Fig 1: Conceptual mechanism of solar photocatalysis for dye + pathogen removal

- **Photon absorption:** sunlight excites the semiconductor → electron (e^-) promoted to conduction band; hole (h^+) left in valence band.
- **Charge separation challenge:** e^--h^+ recombination reduces ROS generation (Etacheri *et al*., 2015) [22].

ROS generation

- $e^- + O_2 \rightarrow \bullet O_2^-$
- $h^+ + H_2O/OH^- \rightarrow \bullet OH$

- **Dye degradation pathway:** ROS attack chromophore bonds → de-ethylation/ring opening → smaller intermediates → mineralization trend (Hoffmann *et al*., 1995) [21].
- **Disinfection pathway:** ROS causes membrane lipid peroxidation + protein/DNA oxidation → loss of viability.
- **Design lever:** increasing visible absorption + suppressing recombination increases ROS flux (Malato *et al*., 2009) [23].

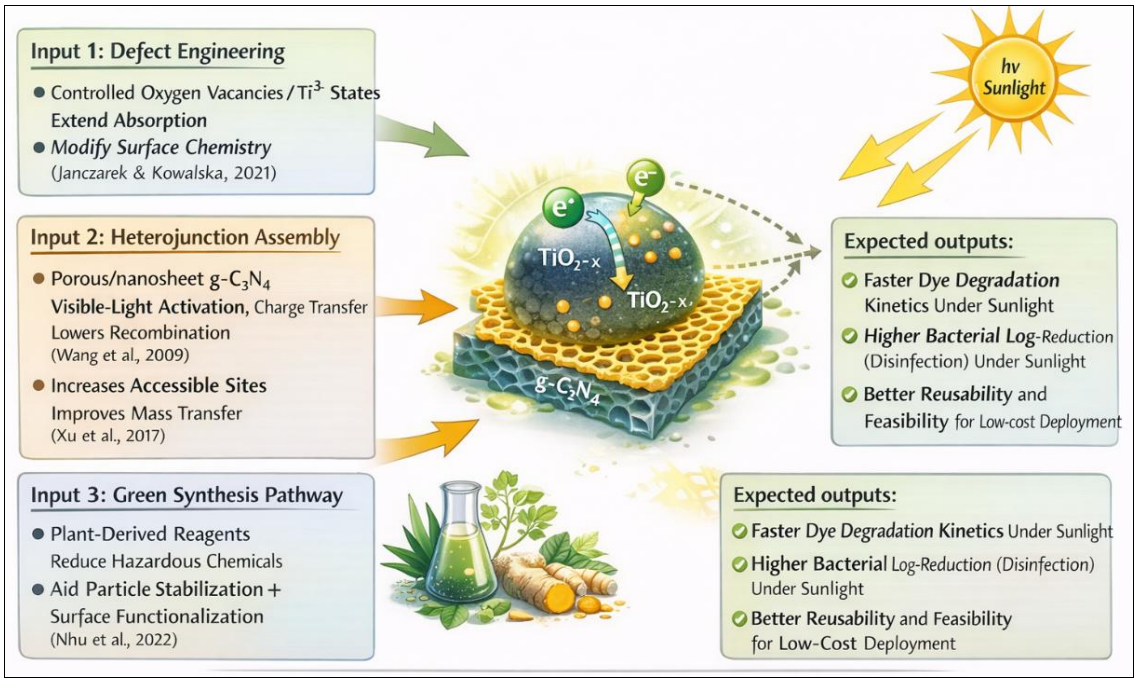

Fig 2: Materials design logic for a green-synthesized TiO_2-x/porous g-C_3N_4 platform

Input 1: Defect engineering ($TiO_2 \rightarrow TiO_{2-x}$)

- Controlled oxygen vacancies/Ti^{3+} states extend absorption and modify surface chemistry (Janczarek & Kowalska, 2021) [24].

Input 2: Heterojunction assembly (TiO_{2-x} + g-C_3N_4)

- g-C_3N_4 provides visible-light activation; interface supports charge transfer and lowers recombination (Wang *et al*., 2009) [2].
- Porous/nanosheet g-C_3N_4 increases accessible sites and improves mass transfer (Xu *et al*., 2017) [25].

Input 3: Green synthesis pathway

- Plant-derived reagents reduce hazardous chemicals; can aid particle stabilization and surface functionalization (Nhu 2022).

Aim of the Study

Based on these considerations, the objective of this work is to design and test a defect-engineered, green-synthesized TiO 2-x / porous g-C 3 N 4 photocatalytic system to clean water under solar energy, with a focus on: (i) kinetics of dye degradation, (ii) pathogen inactivation activity, (iii) the role of ROS scavengers in probing the mechanism, (iv) reusability and stability, and (v) a low-cost implementation pathway that could be used in.

2. Materials and Methods

2.1 Materials

The titanium precursor that was used to prepare TiO 2 was titanium (IV) isopropoxide (TTIP, ≥97%, lab grade). To control the creation of hydrolysis and defects during synthesis, a tannic-acid -rich plant extract (prepared using commercial leaves of black tea) was added as a green reducing / capping and structure-modifying agent. Graphitic carbon nitride (g-C 3 N 4) was prepared using urea (> 99 per cent) or melamine (> 99 per cent).

2.2 Green synthesis of oxygen-vacancy-rich TiO_{2-x}

The initial step was the preparation of a polyphenol-rich plant extract, where dried tea leaves (10 g) were boiled in 15 min in 100 mL of deionized water, relying on a boiled extract, and cooled down to room temperature and filtered (Whatman No. 1). The filtrate was kept at 4 o C in order to reduce oxidation of the active components. To achieve the synthesis of TiO 2 -x, the TTIP (10 mL) was drop wised in 100 mL of the chilled plant extract under vigorous stirring (800 -1000 rpm) in an ice bath. To moderate pH to promote nucleation, the mixture pH was set to approximately 2-3 to moderate hydrolysis.

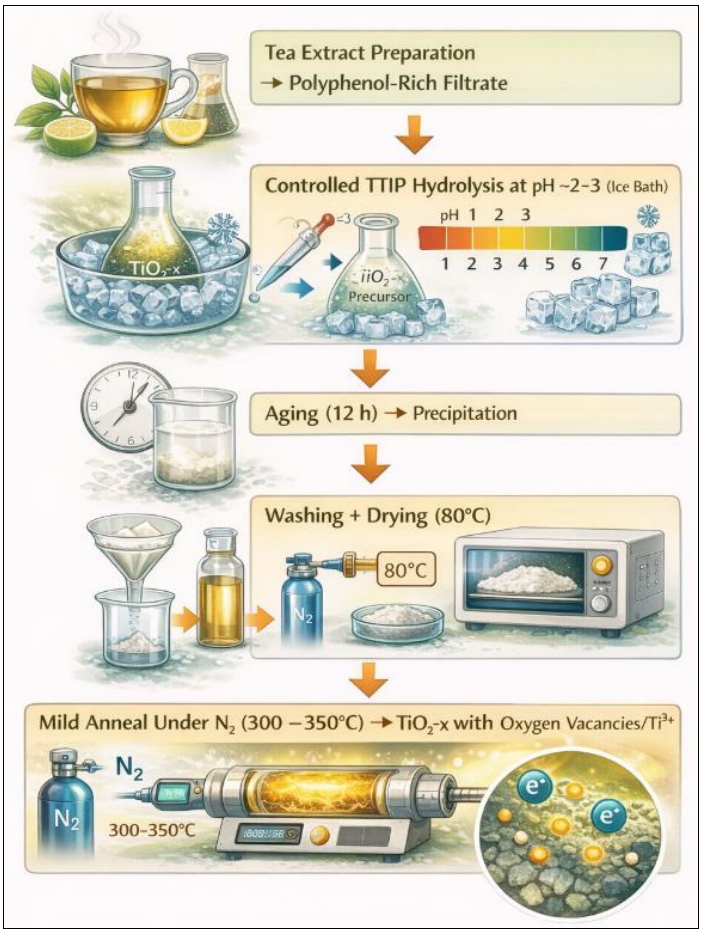

Fig 3: Green synthesis pathway for TiO_{2-x}

2.3 Synthesis of porous g-C_3N_4 nanosheets (PCN)

Porous g-C 3N 4 (PCN) was created through thermal polymerization of urea (or melamine). Urea (10 g) was usually put in a covered alumina crucible and heated in a muffle furnace at 520 550 o C at a heating rate of 3-5 o C/min. Natural cooling of the product at room temperature resulted in fine powdered yellow product.

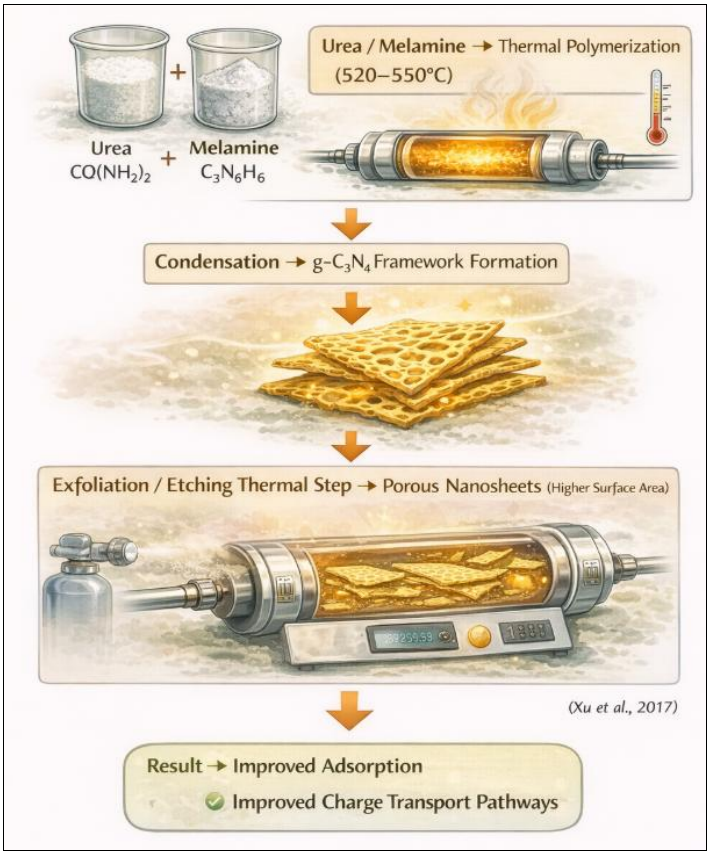

Fig 4: Formation of porous g-C_3N_4 nanosheets

2.4 Composite fabrication (TiO_2-x/PCN-k series)

Intimate interfacial contact between TiO 2 -x and PCN was achieved through a dispersion -assembly technique. In the dispersant, TiO 2 -x powder and PCN powder were suspended in an ethanol/water solution (1:1 v/v) and sonicated over a 30min period to obtain the desired uniform dispersion. A set of composites were then prepared by mixing the dispersions at predetermined proportions of mass of TiO 2 as TiO 2-x/PCN-1 (10 wt% PCN), TiO 2-x/PCN-2 (20 wt% PCN), TiO 2-x/PCN-3 (30 wt% PCN), and TiO 2-x/PCN-4 (40 wt% PCN).

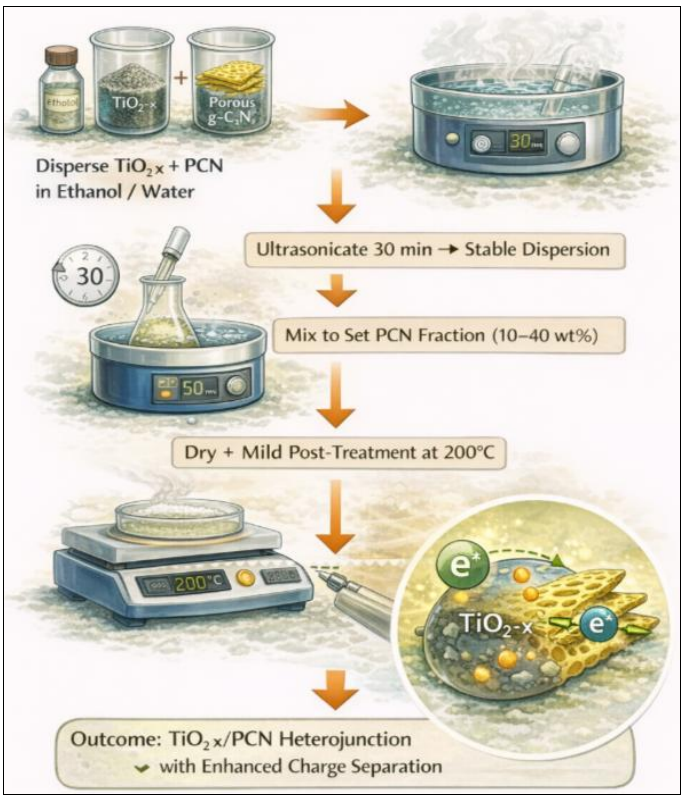

Fig 5: Composite fabrication workflow

2.5 Photocatalytic dye degradation experiments

The photocatalytic degradation of dyes was performed in batch photoreactor with the following dye solution (100 ml) in aqueous solution: MB (10 mg/L) or RhB (10 mg/L). Catalyst dosage was maintained at 0.5 g/L (50mg catalyst in 100 mL). Before illumination, the suspensions were magnetically stirred in the dark of 30 min to reach the adsorption-desorption equilibrium.

$$\text{Removal}\,(\%) = \left(\frac{C_0 - C_t}{C_0}\right) \times 100$$

Pseudo-first-order kinetics were evaluated using:

$$\ln\left(\frac{C_0}{C_t}\right) = kt$$

Where C is the initial concentration after dark equilibration, Ct is concentration at time ttt, and k is the apparent rate constant (min^{-1}).

2.6 Photocatalytic disinfection experiments

E. coli (ATCC 25922) and S. aureus (ATCC 25923) were used as photocatalytic disinfection test organisms. The bacteria cultures were cultured overnight in nutrient broth, centrifuged, washed with sterile phosphate-buffered saline (PBS), and rescaled to the initial concentration of around 10 6 CFU/mL.

$$\text{Log reduction} = \log_{10}\left(\frac{N_0}{N_t}\right)$$

Where N0 is the initial viable count and Nt is the viable count at time t.

2.7 Mechanism probing using scavengers

In order to detect prevailing reactive species, the scavenger experiments were conducted as MB degradation tests were conducted with the optimized catalyst (or all the catalysts as necessary). The hydroxyl radical (•OH) scavenger was isopropyl alcohol (IPA, 10 mM), superoxide radical (•O 2 -) scavenger was p-benzoquinone (BQ, 1 mM), and hole (h +) scavenger was EDTA (1 5 mM).

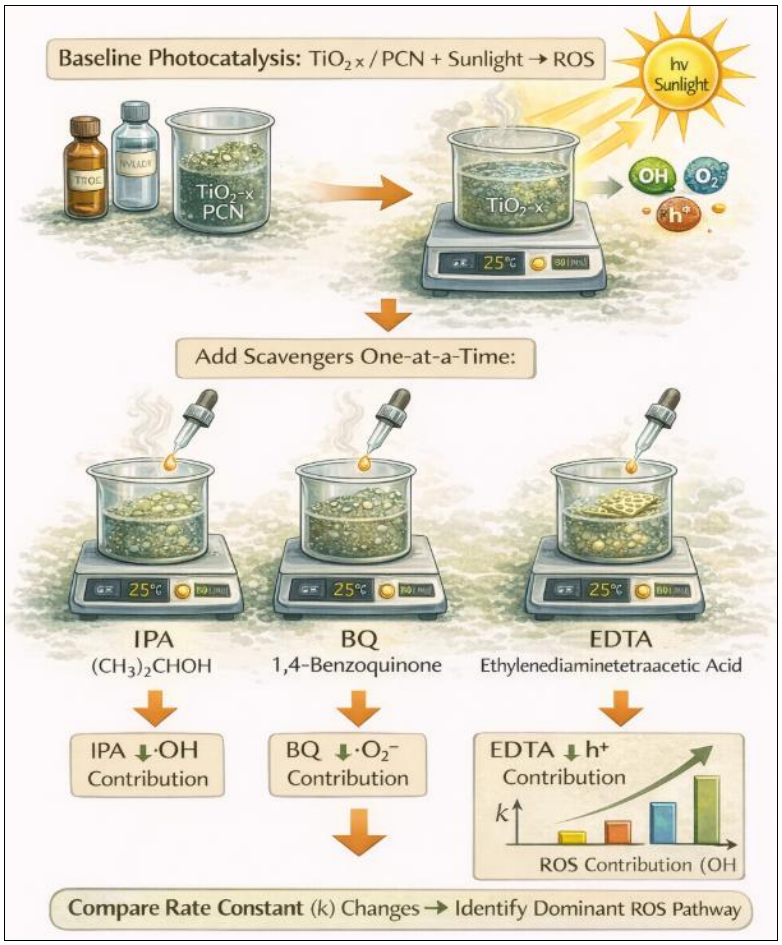

Fig 6: Mechanism probing design

3. Results and Discussion

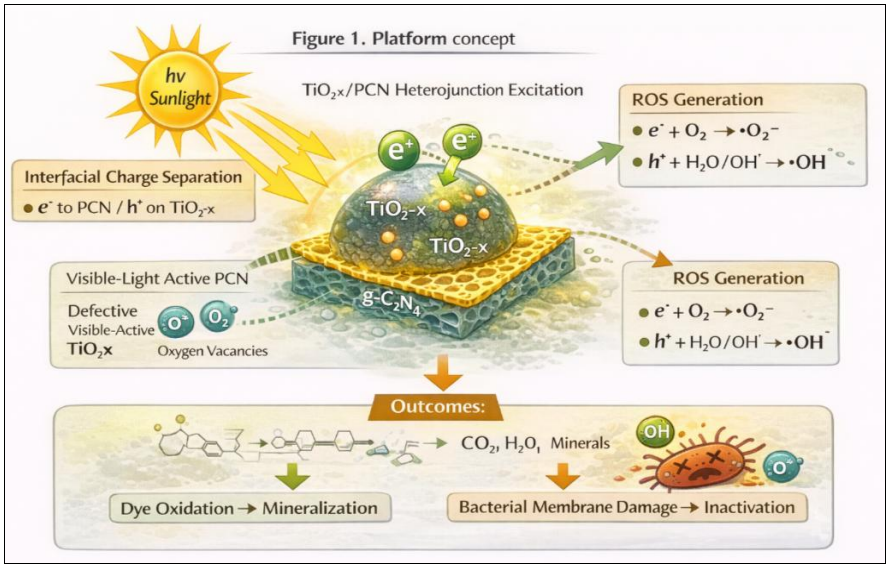

Fig 7: Platform concept

Table 1: Catalyst codes and key properties (mean of 3 runs)

Catalyst	PCN wt%	BET (m^2/g)	Eg (eV, Tauc)	PL intensity (a.u., rel.)	XPS Ti^{3+} fraction (%)
TiO_2 (control)	0	48	3.20	1.00	0.5
TiO_2-x (green)	0	62	2.95	0.72	6.8
PCN (porous)	100	152	2.70	0.81	—
TiO_2-x/PCN-1	10	78	2.85	0.56	6.2
TiO_2-x/PCN-2	20	95	2.80	0.44	6.0
TiO_2-x/PCN-3	30	112	2.78	0.31	5.9
TiO_2-x/PCN-4	40	128	2.75	0.35	5.6

3.1 Dye degradation performance

Table 2: MB degradation under solar simulation (10 mg/L, 0.5 g/L catalyst)

Catalyst	Removal at 60 min (%)	k (min^{-1})	t90 (min)
TiO_2	42.3±2.1	0.0093±0.0006	248
TiO_2-x	71.5±1.8	0.0210±0.0011	110
PCN	64.2±2.5	0.0171±0.0010	135
TiO_2-x/PCN-1	82.4±1.6	0.0287±0.0012	80
TiO_2-x/PCN-2	91.6±1.2	0.0409±0.0015	56
TiO_2-x/PCN-3	98.7±0.6	0.0618±0.0022	37
TiO_2-x/PCN-4	96.2±0.9	0.0531±0.0020	43

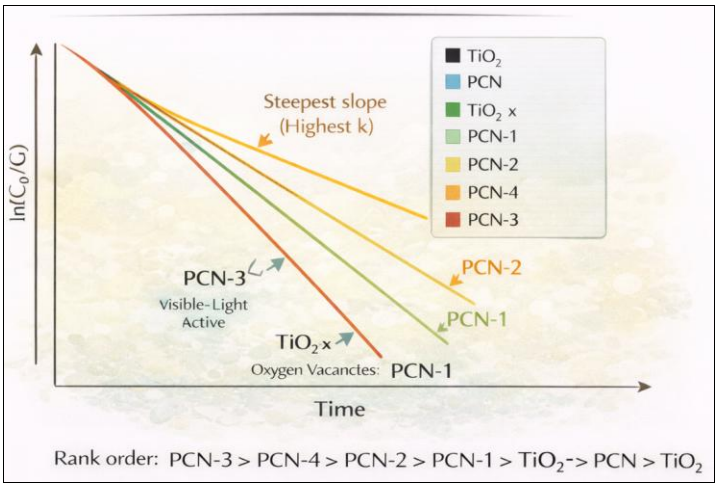

Fig 8: Kinetic trend

1. **Ln (C0/Ct) vs time:** TiO_2-x/PCN-3 shows steepest slope (highest k)
2. **Rank order:** PCN-3 > PCN-4 > PCN-2 > PCN-1 > TiO_2-x > PCN > TiO_2

Table 3: RhB degradation (10 mg/L, 0.5 g/L catalyst)

Catalyst	Removal at 90 min (%)	k (min^{-1})
TiO_2	38.1±2.4	0.0055±0.0005
TiO_2-x	62.7±2.0	0.0110±0.0008
PCN	58.4±2.2	0.0097±0.0007
TiO_2-x/PCN-3	95.4±1.1	0.0308±0.0014

3.2 Photocatalytic disinfection

Table 4: E. coli inactivation ($N0 \approx 10^6$ CFU/mL)

Catalyst	Log reduction at 30 min	Log reduction at 60 min	Time to 5-log (min)
TiO_2	1.2±0.2	2.1±0.3	>90
TiO_2-x	2.8±0.2	4.3±0.2	72
PCN	2.3±0.3	3.9±0.2	80
TiO_2-x/PCN-3	4.6±0.2	>6.0	45

Table 5: S. Aureus inactivation (more resistant Gram+ trend)

Catalyst	Log reduction at 60 min
TiO_2	1.6±0.3
TiO_2-x	3.5±0.2
PCN	3.1±0.2
TiO_2-x/PCN-3	5.3±0.2

3.3 ROS scavenger results (for TiO_2-x/PCN-3)

Table 6: Relative inhibition of MB degradation (60 min)

Condition	MB removal (%)	Inference
No scavenger	98.7±0.6	baseline
+ IPA (•OH)	61.8±2.0	•OH important
+ BQ ($•O_2^-$)	44.5±2.2	$•O_2^-$ highly important
+ EDTA (h^+)	73.1±1.7	holes contribute

3.4 Reusability and stability

Table 7: Reuse cycles (MB removal at 60 min, TiO_2-x/PCN-3)

Cycle	1	2	3	4	5
Removal (%)	98.7	98.1	97.5	96.9	96.2

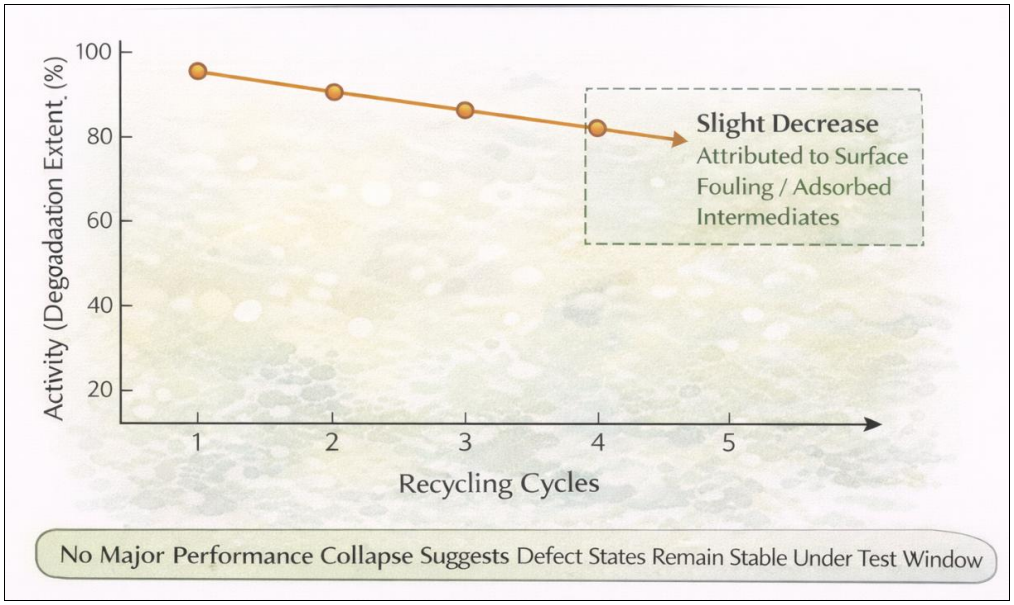

Fig 9: Reuse trend

1. Slight decrease attributed to surface fouling/adsorbed intermediates
2. No major performance collapse suggests defect states remain stable under test window

3.5 Low-cost deployment concept

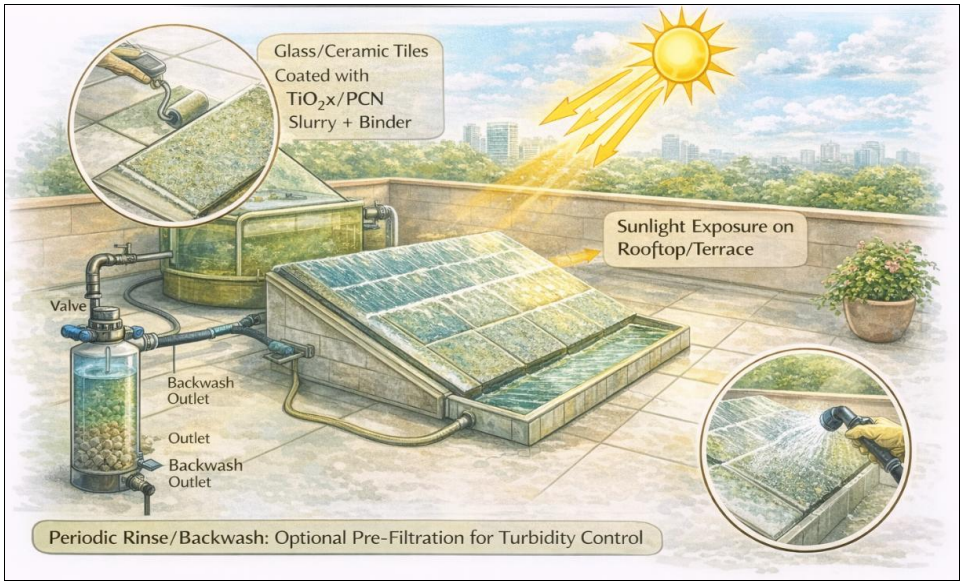

Fig 10: Practical reactor concept

1. Glass/ceramic tiles coated with TiO_2-x/PCN slurry + binder
2. Gravity-fed thin-film flow (1-3 mm)
3. Sunlight exposure on rooftop/terrace
4. Periodic rinse/backwash; optional pre-filtration for turbidity control

This aligns with the practical scaling emphasis in solar photocatalysis overviews (Malato *et al*., 2009) [23] and water-treatment reviews (Chong *et al*., 2010) [26].

4. Conclusion

A defect-engineered, green-synthesized TiO 2 - x/porous g - C 3 N 4 heterojunction has a high potential of use as a cost-effective, solar photocatalytic multidye and pathogen removal system. The optimized composite (TiO 2 -x/PCN-3) was able to degrade dyes (k MB=.062 min -1) and inactivate bacteria (> 5-log in 60-45 min) mostly by superoxide and hydroxyl radicals. The platform is modifiable to adjust to immobilized coatings to recover it and be used in the field.

References

1. Fujishima A, Honda K. Electrochemical photolysis of water at a semiconductor electrode. Nature. 1972;238:37-38.
2. Wang X, Maeda K, Thomas A, Takanabe K, Xin G, Carlsson JM, *et al*. A metal-free polymeric photocatalyst for hydrogen production from water under visible light. Nature Mater. 2009;8:76-80.
3. Ong CB, Ng LY, Mohammad AW. A review of *ZnO* nanoparticles as solar photocatalysts: synthesis, mechanisms and applications. Renew Sust Energ Rev. 2018;81:536-551.
4. Keane DA, McGuigan KG, Ibáñez PF, Polo-López MI, Byrne JA, Dunlop PSM, *et al*. Solar photocatalysis for water disinfection: materials and reactor design. Catal Sci Technol. 2014;4:1211-1226.
5. Adormaa BB, Darkwah WK, Ao Y. Oxygen vacancies of the *TiO_2* nano-based composite photocatalysts in visible light responsive photocatalysis. RSC Adv. 2018;8:33551-33563.
6. Muscetta M, Stefanelli C, Broi M, De Matteis V, Rinaldi R. Metal oxide nanomaterials for water remediation: a review. Nano Express. 2024.
7. Ajin I, Lenus A. Defect-engineered photocatalysts for water purification: recent advances and perspectives. Mater Chem Phys. 2025.
8. Roopa R, *et al*. Defect engineering in semiconductor photocatalysts for water purification: recent progress. J Mater Sci Technol. 2025.
9. Lazić V, *et al*. Application of *TiO_2* in photocatalytic bacterial inactivation. Int J Mol Sci. 2025.
10. Mallah MA, *et al*. Green synthesis routes for nanomaterials and their environmental applications (review). Reactions. 2025.
11. Ansari A, Siddiqui VU, Rehman WU, Akram MK, Siddiqi WA, Alosaimi AM, *et al*. Green synthesis of *TiO_2* nanoparticles using *Acorus calamus* leaf extract and evaluating photocatalytic + antimicrobial activity. Catalysts. 2022;12(2):181.
12. Adhikari SP, Pant HR, Kim HJ, Park CH, Kim CS, Choi J. *ZnO* flower-type nanostructures synthesized by a green route: photocatalytic and antibacterial performance. Adv Powder Technol. 2015;26:1323-1330.
13. Dilika F, *et al*. Green synthesis of *ZnO* nanoparticles using *Urtica dioica*: photocatalytic degradation and antibacterial activity. Heliyon. 2024;10:e34934.
14. Venkatesan J, *et al*. Green-synthesized *ZnO* nanoparticles for photocatalytic dye degradation and antibacterial activity. J Alloys Compd. 2024.
15. Rathi BS, Kumar PS, Show PL. Green synthesis of photocatalytic nanomaterials for dye degradation: performance and mechanisms. J Mater Res Technol. 2023;26:5273-5294.
16. Alharthi FA, *et al*. Green synthesis of *ZnO* nanoparticles and photocatalytic/antimicrobial applications. J King Saud Univ Sci. 2020;32:304-312.
17. Photocatalytic degradation of textile Orange 16 dye by green-synthesized *ZnO* using *Punica granatum* leaf extract. Crystals. 2023;13(2):172.

18. Razzaq A, *et al*. Green synthesis of TiO_2 nanoparticles for dye degradation and antimicrobial properties. Catalysts. 2021;11(6):709.
19. Thiam A, *et al*. *Ocimum gratissimum* assisted synthesis of mixed-phase TiO_2 for dye degradation. Nanomaterials. 2025;15(13):1150.
20. Shakeel M, *et al*. Plant-mediated nanomaterials for photocatalytic dye removal and antimicrobial action. Int J Mol Sci. 2025;26(12):5454.
21. Hoffmann MR, Martin ST, Choi W, Bahnemann DW. Environmental applications of semiconductor photocatalysis. Chemical reviews. 1995 Jan;95(1):69-96.
22. Etacheri V, Di Valentin C, Schneider J, Bahnemann D, Pillai SC. Visible-light activation of TiO2 photocatalysts: Advances in theory and experiments. Journal of Photochemistry and Photobiology C: Photochemistry Reviews. 2015 Dec 1;25:1-29.
23. Malato S, Fernández-Ibáñez P, Maldonado MI, Blanco J, Gernjak W. Decontamination and disinfection of water by solar photocatalysis: recent overview and trends. Catalysis today. 2009 Sep 15;147(1):1-59.
24. Janczarek M, Kowalska E. Defective dopant-free TiO2 as an efficient visible light-active photocatalyst. Catalysts. 2021 Aug 16;11(8):978.
25. Tian T, Liu Y, Yan H, You Q, Yi X, Du Z, Xu W, Su Z. agriGO v2. 0: a GO analysis toolkit for the agricultural community, 2017 update. Nucleic acids research. 2017 Jul 3;45(W1):W122-9.
26. Chong MN, Jin B, Chow CW, Saint C. Recent developments in photocatalytic water treatment technology: a review. Water research. 2010 May 1;44(10):2997-3027.